

## The influence of methanesulfonate ions on physico-chemical properties of lead dioxide

Alexander VELICHENKO<sup>1\*</sup>, Tatiana LUK'YANENKO<sup>1</sup>, Olesia SHMYCHKOVA<sup>1</sup>, Pavlo DEMCHENKO<sup>2</sup>, Roman GLADYSHEVSKI<sup>2</sup>

<sup>1</sup> Ukrainian State University of Chemical Technology, Gagarine Ave. 8, 49005 Dnipro, Ukraine

<sup>2</sup> Department of Inorganic Chemistry, Ivan Franko National University of Lviv, Kyryla i Mefodiya St. 6, 79005 Lviv, Ukraine

\* Corresponding author. Tel.: +380567462825; e-mail: velichenko@ukr.net

Received May 28, 2021; accepted June 30, 2021; available on-line December 1, 2021  
<https://doi.org/10.30970/cma14.0413>

**The results of an investigation of the influence of methanesulfonate ions on physico-chemical properties of electrochemically deposited lead dioxide are reported. It was possible to synthesize high-quality films of up to 2 mm thickness, free from internal stress, with reliable adhesion to the substrate in the current density range 2-180 mA·cm<sup>-2</sup>. Changes in the composition of the methanesulfonate electrolyte or the deposition conditions affected the relative contents of the  $\alpha$ - and  $\beta$ -modifications of the dioxide. The main difference, compared with lead oxides obtained from nitrate solutions, was the significant amount of  $\alpha$ -phase, which varied from 17 to 90%. The deposits were well crystallized and contained smaller crystals.**

Lead(IV) oxide / Methanesulfonate ion / Phase composition / Current efficiency

### 1. Introduction

The use of various technologies for back-up energy storage makes it possible to solve a number of important problems on a global scale, in particular, ensure the possibility of continuous use of a number of non-traditional environmentally friendly methods of generating electricity [1], for example, wind generators [2] and solar panels [3,4]. At the moment, several fundamentally different possibilities of reserve energy storage are known, one of which is the use of chemical transformations in secondary power sources [5,6]. There are several types of chemical power source that may be of potential interest when used as backup energy storage devices: stationary batteries (lead batteries, nickel-cadmium and nickel-metal hydride batteries) [7] and flow redox batteries [8]. The latter are the most attractive and promising ones, since they are relatively small in size, can be built according to a modular type (unification of production, flexibility in building storage units of required power from standard elements), they can be easily transported and maintained. Lead-acid batteries find their application in the maintenance of modern household and industrial equipment and are installed in cars. The main advantages of this type of battery are its low cost, simple and well-known technological

process, almost 100% effective recycling, and low self-discharge. The disadvantages include a limited number of full charge/discharge cycles, a need for storage in charged condition and the high mass caused by a low specific energy in comparison with newer battery types, among which the soluble lead redox flow battery is recognized as of particular interest. It makes use of the variable oxidation states of lead, namely Pb, Pb(II) and Pb(IV). Electrolytes are designed either from lead oxide, lead carbonate or aqueous lead methanesulfonate, and methanesulfonic acid [9].

Lead dioxide is widely used in electrochemical industry and is regarded as a promising electrode [10] due to its low cost compared to noble metals, high chemical stability and catalytic activity in oxygen transfer reactions. In this context, here we present a thorough study of the influence of deposition conditions on the structure and phase composition of PbO<sub>2</sub> formed by electrodeposition from methanesulfonic acid media.

### 2. Experimental

All the chemicals used here were reagent grade. The regularities of lead dioxide electrodeposition were

studied on a Pt rotating disk electrode (Pt-RDE, 0.19 cm<sup>2</sup>) by steady-state voltammetry. For the RDE experiments a voltammetry system SVA-1BM was used. The potential scan rate was varied within 1–100 mV/s, depending on the purpose of the experiment. Before each experiment, the electrode surface was treated with a freshly prepared mixture (1:1) of concentrated H<sub>2</sub>SO<sub>4</sub> and H<sub>2</sub>O<sub>2</sub>. This preliminary treatment technique stabilizes the electrode surface, which under the action of a strong oxidizing medium is oxidized to a certain state (defined phase and chemical composition of the surface oxides), which ensures satisfactory reproducibility in recording cyclic voltammograms in the background electrolyte (0.1 M CH<sub>3</sub>SO<sub>3</sub>H). Voltammetry measurements were carried out in a standard temperature-controlled three-electrode cell. All potentials were recorded and reported vs. Ag / AgCl / KCl<sub>(sat.)</sub>.

X-ray powder diffraction (XRPD) data were collected in the transmission mode on a STOE STADI P diffractometer with Cu K $\alpha$ <sub>1</sub>-radiation, a curved Ge (1 1 1) monochromator on the primary beam, 2 $\theta$ -scan, angular range for data collection 20.000–110.225 °2 $\theta$  with an increment of 0.015, linear position-sensitive detector with a step of 0.480 °2 $\theta$  and time per step 75–300 s, U = 40 kV, I = 35 mA, T = 298 K. A calibration procedure was performed using SRM 640b (Si) and SRM 676 (Al<sub>2</sub>O<sub>3</sub>) NIST standards. Preliminary data processing and X-ray qualitative phase analysis were performed using STOE WinXPOW and PowderCell program packages [11]. The crystal structures of the phases were refined by the Rietveld method with the program FullProf.2k, applying a pseudo-Voigt profile function and isotropic approximation for the atomic displacement parameters, together with quantitative phase analysis [12,13].

The current efficiency (CE) of the lead dioxide deposition was determined by coulometrically measuring the total charge (Q) passed during electrolysis. Subsequently, the charge passed for the cathodic reduction (Q<sub>red</sub>) of pre-formed PbO<sub>2</sub> was also measured coulometrically in the background electrolyte. As has been shown earlier [14], at slow sweep rates, quantitative reduction of PbO<sub>2</sub> takes place for thin oxide films. For relatively thick films, the adequacy of the method was confirmed by gravimetric experiments that showed a direct proportionality between charge and amount of deposited PbO<sub>2</sub>, as reported in the above cited publications. The current efficiency for PbO<sub>2</sub> formation was calculated from the reduction charge divided by the total charge according to the following formula:

$$CE = \frac{Q_{\text{red}}}{Q} \cdot 100\%$$

### 3. Results and discussion

The formation of lead dioxide proceeds simultaneously with oxygen evolution [15]. Since the current efficiency decreases with increasing PbO<sub>2</sub> deposition potential, the potential range in which PbO<sub>2</sub> formation is the predominant process is small. The knowledge of the dependence of PbO<sub>2</sub> CE on various factors is important for selecting the optimal electrolyte composition and deposition conditions. A typical dependence of CE on the current density is shown in Fig. 1. The dependence is extreme, which is associated with the simultaneous formation of lead(IV) oxide and oxygen evolution.

At low current densities, when the rate of formation of lead(IV) oxide is negligible, the oxide coating is not continuous and the oxygen evolution reaction (OER) can take place on oxide-free portions of the platinum, where the OER overvoltage is substantially lower than on PbO<sub>2</sub>. Increase of the current density contributes to fast filling of the platinum electrode surface with lead(IV) oxide; the OER overvoltage increases and CE approaches 100%. Thus, in the area I (see Fig. 1), where CE increases with increasing current density, the process simultaneously proceeds allegedly on both electrodes, platinum and lead dioxide, with a gradually complete transition to the latter. In the area II of the curve, the current efficiency is 100% and does not depend on the current density, since oxygen has not yet been released on PbO<sub>2</sub> due to the high overvoltage. The area III of the curve shows a rapid fall in CE due to the fact that the deposition current of the lead dioxide reaches a limit value, while the rate of oxygen evolution increases exponentially.

According to the data obtained here (Fig. 2), by increasing the concentration of lead methanesulfonate (Pb(MS)<sub>2</sub>) it becomes possible to significantly expand the range of current densities at which lead dioxide with 100% current efficiency can be obtained. An additional effect can also be obtained by stirring the electrolyte (see Fig. 2). It should be noted that a change of the amount of methanesulfonic acid (MSA) in the electrolyte within the concentration range from 0.05 to 2.0 M does not affect the current efficiency significantly, which is probably due to the similar effect of the acid on the electrodeposition of PbO<sub>2</sub> and the OER. During the deposition of lead dioxide in the whole investigated current density range, where CE is about 100%, up to 2 mm-thick high-quality deposits with low internal stress and reliable adhesion to the metal substrate (Ti/Pt) were obtained, which may be of potential interest for use as electrocatalytic layer components of DSA<sup>®</sup>.

Crystalline lead dioxide occurs in the form of two different minerals: scrutinyite ( $\alpha$ -PbO<sub>2</sub>) and plattnerite ( $\beta$ -PbO<sub>2</sub>).  $\alpha$ -PbO<sub>2</sub> crystallizes in the orthorhombic structure of Fe<sub>2</sub>N, while  $\beta$ -PbO<sub>2</sub> crystallizes in a tetragonal structure of the rutile type. In both cases, the tetravalent lead ion is located at the center of a distorted octahedron formed by six oxygen ions [16].

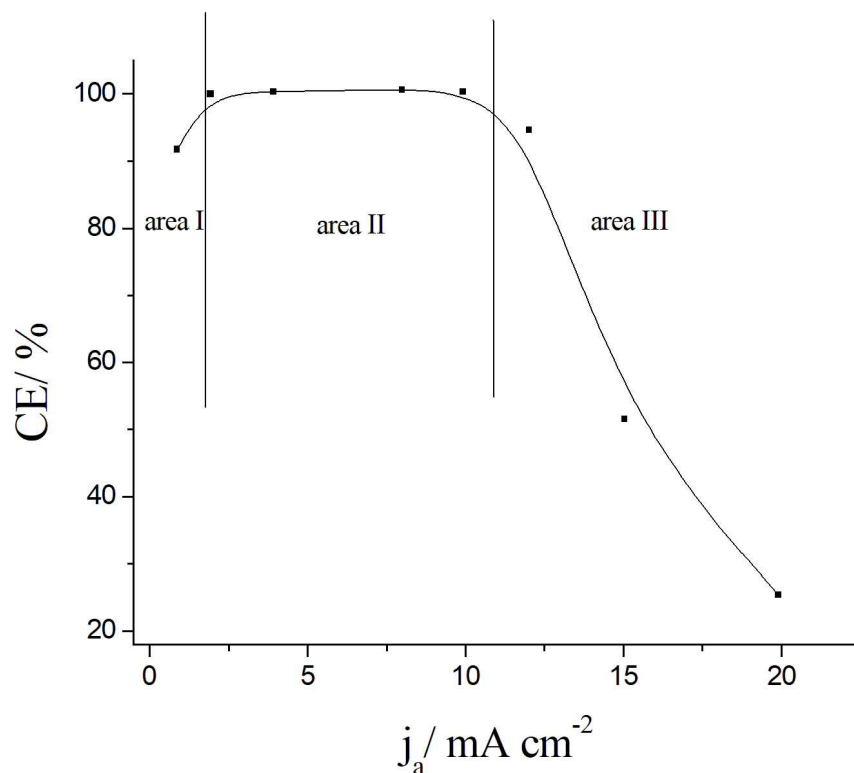


**Fig. 1** Current efficiency of  $\text{PbO}_2$  vs. current density in  $0.1 \text{ M Pb}(\text{CH}_3\text{SO}_3)_2 + 0.1 \text{ M CH}_3\text{SO}_3\text{H}$ .

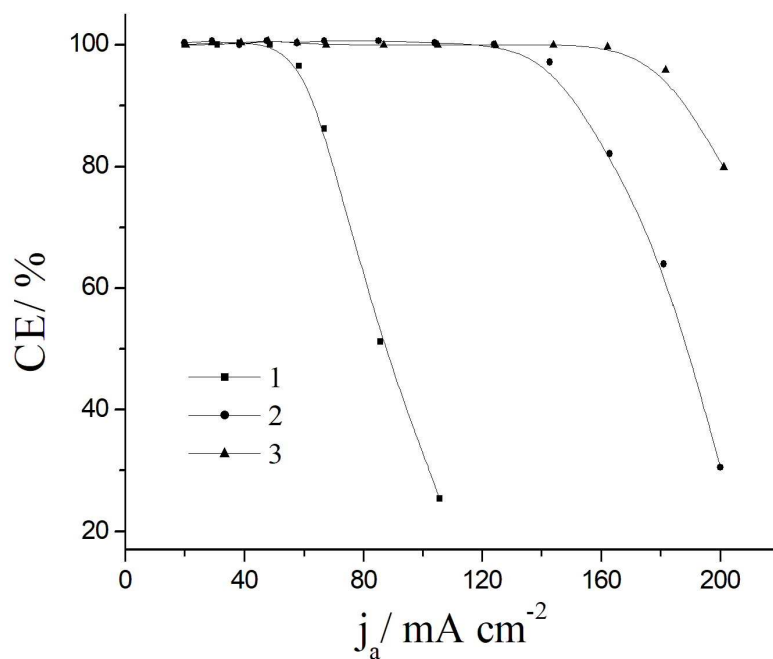


**Fig. 2** Current efficiency of  $\text{PbO}_2$  vs. current density in different electrolytes: 1 –  $0.5 \text{ M Pb}(\text{CH}_3\text{SO}_3)_2 + 0.1 \text{ M CH}_3\text{SO}_3\text{H}$ ; 2 –  $1.0 \text{ M Pb}(\text{CH}_3\text{SO}_3)_2 + 0.1 \text{ M CH}_3\text{SO}_3\text{H}$ ; 3 –  $1.0 \text{ M Pb}(\text{CH}_3\text{SO}_3)_2 + 0.1 \text{ M CH}_3\text{SO}_3\text{H}$  with stirring.

The main difference between these two modifications lies in the arrangement of the octahedra:  $\alpha$ -PbO<sub>2</sub> has a more compact structure, which, however, leads to poor conductivity compared to  $\beta$ -PbO<sub>2</sub> [17]. Usually, electrodeposited coating is composed of different proportions of  $\alpha$ - /  $\beta$ -PbO<sub>2</sub> [18].

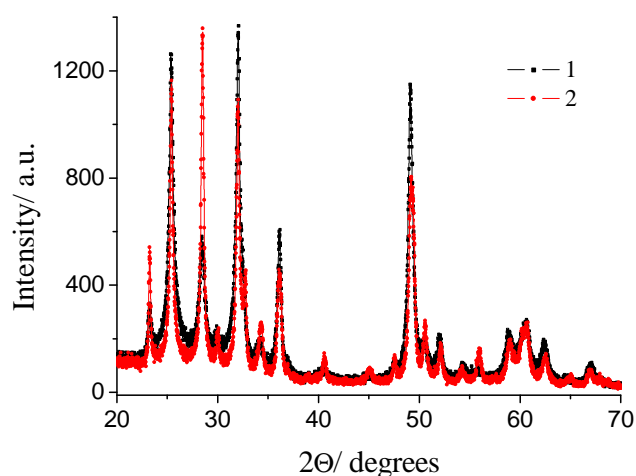
We conducted X-ray powder diffraction in order to investigate the effect of the electrolyte composition and deposition conditions on the phase composition of electrodeposited PbO<sub>2</sub> and its texture. Having in mind the potential impact on the bond strength of oxygen-containing radicals adsorbed on the electrode surface, structural parameters such as the texture and phase composition of PbO<sub>2</sub>-based materials may be important. These factors can also affect the chemical composition of the PbO<sub>2</sub> surface by changing the number and nature of cationic vacancies, as well as the nature and surface concentration of oxygen-containing compounds. Unlike nitrate solutions, the use of methanesulfonate electrolytes of different compositions makes it possible to change the phase composition of the coating over a wide range. First of all, it should be noted that the addition of 0.1 M sodium methanesulfonate (NaMS) to the nitrate electrolyte led to an increase of the content of  $\alpha$ -phase from 15 to 41 % (Table 1). Further increase of the concentration of NaMS hardly affected the phase

composition of the coating. Changing the ratio between the allotropic forms did also not lead to the emergence of new crystallographic orientations of the  $\alpha$ - and  $\beta$ -phases. The observed effect indicates that the amount of methanesulfonate ions available in the phase formation process has a greater effect on the adsorption than on the complexation. As has been shown in our previous publication [19], at such concentrations the ratio of ligand to lead ions, even at maximum NaMS concentrations in the solution, almost a quarter of the Pb<sup>2+</sup> ions remain free, and the complex formed is predominantly a single charge cation. 0.1 M NaMS concentration in the electrolyte is sufficient to achieve maximum adsorption.

As can be seen from the X-ray diffractograms shown in Fig. 3, in the presence of 0.1 M NaMS in the nitrate electrolyte, the coating texture changes slightly. The same reflections were observed for the PbO<sub>2</sub> coatings obtained from nitrate and methanesulfonate baths, however, the intensity of some of them changed when methanesulfonate ions were added into the solution. There was a significant increase of the intensities of the reflections (1 1 0)  $2\theta = 23.30^\circ$  and (1 1 1)  $2\theta = 28.50^\circ$  for the  $\alpha$ -phase, as well as a decrease of the intensities of the reflections (1 1 0)  $2\theta = 25.40^\circ$ ; (0 1 1)  $2\theta = 31.90^\circ$ ; (0 2 0)  $2\theta = 36.20^\circ$ , and (1 2 1)  $2\theta = 49.10^\circ$  for the  $\beta$ -phase.

**Table 1** Phase composition of PbO<sub>2</sub> for different methanesulfonate concentrations in mixed deposition electrolytes.

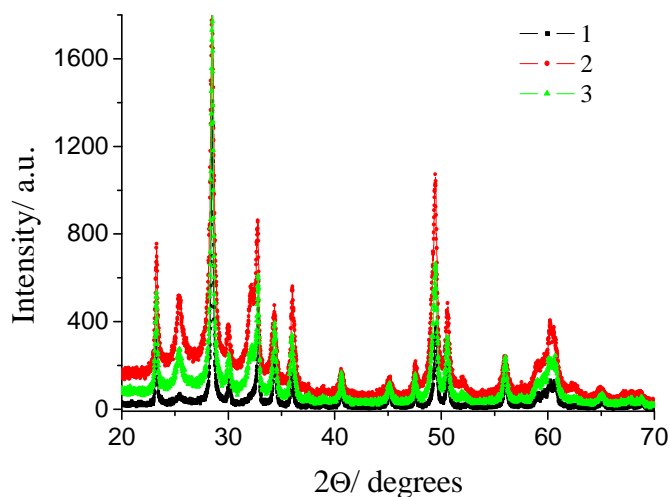
Electrolyte	$\alpha$ -PbO <sub>2</sub> / %	$\beta$ -PbO <sub>2</sub> / %
0.1 M Pb(NO <sub>3</sub> ) <sub>2</sub> + 1.0 M HNO <sub>3</sub> (N)	16	84
(N) + 0.1M NaMS	41	59
(N) + 0.4M NaMS	40	60
(N) + 0.5M NaMS	43	57
(N) + 0.6M NaMS	44	56
(N) + 1.2M NaMS	44	56



**Fig. 3** X-ray diffractograms of PbO<sub>2</sub> coatings electrodeposited at  $j_a = 5 \text{ mA}\cdot\text{cm}^{-2}$  and 25 °C from the following solutions: 1 – 0.1 M Pb(NO<sub>3</sub>)<sub>2</sub> + 1.0 M HNO<sub>3</sub>; 2 – 0.1 M Pb(NO<sub>3</sub>)<sub>2</sub> + 1.0 M HNO<sub>3</sub> + 0.1 M NaMS.

**Table 2** Phase composition of PbO<sub>2</sub> for different electrolytes and coating thicknesses.

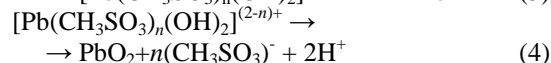
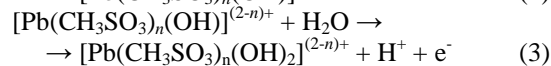
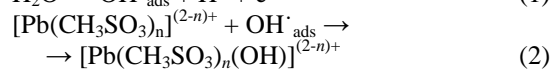
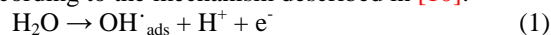
Electrolyte	$\alpha$ -PbO <sub>2</sub> / %	$\beta$ -PbO <sub>2</sub> / %
0.1 M Pb(MS) <sub>2</sub> + 0.1 M MSA; 50 $\mu$ m	17	83
0.1 M Pb(MS) <sub>2</sub> + 0.1 M MSA; 500 $\mu$ m	21	79
0.1 M Pb(MS) <sub>2</sub> + 1.0 M MSA; 50 $\mu$ m	90	10
0.1 M Pb(MS) <sub>2</sub> + 1.0 M MSA; 500 $\mu$ m	60	40

**Fig. 4** X-ray diffractograms of PbO<sub>2</sub> coatings of different thicknesses, electrodeposited at  $j_a = 10 \text{ mA}\cdot\text{cm}^{-2}$  and 25 °C from 0.1 M Pb(MS)<sub>2</sub> + 1.0 M MSA, where 1 – 50; 2 – 500; 3 – 1000  $\mu$ m.

According to the results obtained here (Table 2), the phase composition of the coating depends on the thickness and on the content of methanesulfonic acid in the electrolyte. At low concentrations (0.1 M), a tenfold increase of the coating thickness (up to 500  $\mu$ m) led to a slight decrease of the  $\beta$ -phase content (by 4 %), *i.e.*, for systems of this type, the dependency of the phase composition on the coating thickness can be neglected. The texture of the obtained coatings is also nearly the same. A significantly different situation was observed for the deposition from electrolytes with a high concentration of methanesulfonic acid (1.0 M). A similar tenfold increase of the coating thickness resulted in a significant decrease of the content of  $\alpha$ -phase (up to 60 %). However, further increase of the coating thickness up to 1000  $\mu$ m did not change the phase composition of the coating. The texture of the coatings of different thicknesses also remained virtually unchanged (Fig. 4). The intensities of the (1 1 0), (0 1 1) and (1 2 1) reflections of the  $\beta$ -phase increased significantly, which indicated higher content of this modification.

Increasing the current density from 5 to 10  $\text{mA}\cdot\text{cm}^{-2}$  had virtually no effect on the phase composition and texture of the coatings, while increasing the acid content of both nitrate and methanesulfonate solutions from 0.1 M to 1.0 M

produced a significant increase of the amount of  $\alpha$ -phase in the coating, up to 25 and 90 %, respectively. Under these conditions, the  $\alpha$ -phase becomes the main phase of the lead dioxide obtained from the methanesulfonate medium. It should be noted that at low acidity, the phase compositions of PbO<sub>2</sub> synthesized from nitrate and methanesulfonate electrolytes are very similar. However, at 1.0 M concentration of acid in mixed nitrate-methanesulfonate electrolytes, the maximum amount of  $\alpha$ -phase is only 44 %, which is twice lower than for the methanesulfonate electrolyte with the same concentration of lead and methanesulfonate ions. Since the nitrate ion is not adsorbed on the electrode surface and does not form complex compounds with Pb<sup>2+</sup>, the presence of sodium ions in the solution may be the only effect. The latter affect the composition and structure of the intermediate oxygen-containing Pb(III) and Pb(IV) compounds, which are formed at steps (2) and (3) of the PbO<sub>2</sub> electrodeposition according to the mechanism described in [10]:



The initial step of the process is the electrooxidation of water with the formation of oxygen-containing radicals of  $\text{OH}^{\text{ads}}$  type on the electrode surface (1). Considering the water concentration in aqueous solutions and the fact that the hydroxylation of the electrode surface occurs at much lower potentials than the processes of oxygen evolution and oxidation of lead compounds, this stage is rapid. Then follows the chemical stage of oxidation of  $[\text{Pb}(\text{CH}_3\text{SO}_3)_n]^{(2n)+}$  by oxygen-containing radicals  $\text{OH}^{\text{ads}}$  (2) with the formation of (unfixed on the electrode surface) Pb(III) hydroxo complexes  $[\text{Pb}(\text{CH}_3\text{SO}_3)_n(\text{OH})]^{(2-n)+}$ , which are subsequently (3) oxidized at the electrochemical step of the charge transfer. At the last step of the process, the hydroxo complexes of tetravalent lead decay by a chemical mechanism with the formation of lead dioxide (4).

The above mentioned  $[\text{Pb}(\text{CH}_3\text{SO}_3)_n]^{(2n)+}$  and  $[\text{Pb}(\text{CH}_3\text{SO}_3)_n(\text{OH})]^{(2-n)+}$  intermediates are directly involved in the crystallization of  $\text{PbO}_2$ , so their composition and charge are reflected in both the crystallization regularities and the phase composition of the coatings. Reducing the acidity will promote deprotonation of hydroxyl groups, which will facilitate the formation of lead dioxide.

## Conclusions

The addition of 0.1 M sodium methanesulfonate to a nitrate electrolyte led to an increase of the content of the  $\alpha$ -modification of lead dioxide from 15 to 41 %. Further increase of the concentration of NaMS did not affect the phase composition of the coating. Changing the ratio between the allotropic forms did not lead to the emergence of new crystallographic orientations of the  $\alpha$ - and  $\beta$ -phases. The deposits were well crystallized. The maximum X-ray diffraction intensities were observed for the reflections (1 1 0)  $2\theta = 25.40^\circ$ ; (0 1 1)  $2\theta = 31.90^\circ$  and (1 2 1)  $2\theta = 49.10^\circ$  for the  $\beta$ -phase, and (1 1 1)  $2\theta = 28.50^\circ$  for the  $\alpha$ -phase. An increase in the temperature of the methanesulfonate electrolytes leads to an increase in the  $\beta$ -phase content. Stirring the methanesulfonate electrolyte resulted in an increase of the content of  $\alpha$ -phase by 6 % (up to 27 %) with virtually unchanged texture of the coating. There was a decrease of the intensities of the main reflections under stirring, but the coating was characterized by a high degree of crystallinity. Thus, the main factor influencing the phase composition of  $\text{PbO}_2$  obtained from methanesulfonate electrolytes is the concentration of methanesulfonic acid. Changing its concentration in the solution from 0.1 M to 1.0 M made it possible to increase the amount of  $\alpha$ -phase in the coating from 17 to 90 %.

## References

- [1] A. Zuser, H. Rechberger, *Resour., Conserv. Recycl.* 56(1) (2011) 56-65.
- [2] E. Hernandez-Estrada, O. Lastres-Danguillecourt, J.B. Robles-Ocampo, A. Lopez-Lopez, P.Y. Sevilla-Camacho, B.Y. Perez-Sarinana, J.R. Dorrego-Portela, *Renewable Sustainable Energy Rev.* 137 (2021) 110447.
- [3] G. Schileo, G. Grancini, *J. Mater. Chem. C* 9(1) (2021) 67-76.
- [4] W.-J. Yin, J.-H. Yang, J. Kang, Y. Yan, S.-H. Wei, *J. Mater. Chem. A* 3(17) (2015) 8926-8942.
- [5] Y. He, B. Matthews, J. Wang, L. Song, X. Wang, G. Wu, *J. Mater. Chem. A* 6(3) (2018) 735-753.
- [6] L. Dong, C. Xu, Y. Li, Z.-H. Huang, F. Kang, Q.-H. Yang, X. Zhao, *J. Mater. Chem. A* 4(13) (2016) 4659-4685.
- [7] X. Li, F.C. Walsh, D. Pletcher, *Phys. Chem. Chem. Phys.* 13(3) (2011) 1162-1167.
- [8] R.G.A. Wills, J. Collins, D. Stratton-Campbell, C.T.J. Low, D. Pletcher, F.C. Walsh, *J. Appl. Electrochem.* 40(5) (2010) 955-965.
- [9] M. Krishna, E.J. Fraser, R.G.A. Wills, F.C. Walsh, *J. Energy Storage* 15 (2018) 69-90.
- [10] A. Velichenko, T. Luk'yanenko, O. Shmychkova, L. Dmitrikova, *J. Chem. Technol. Biotechnol.* 2020. doi: 10.1002/jctb.6483.
- [11] STOE WinXPOW, version 3.03. Darmstadt: Stoe & Cie GmbH, 2010.
- [12] W. Kraus, G. Nolze, *PowderCell for Windows* (version 2.4) Berlin: Federal Institute for Materials Research and Testing, 2000.
- [13] J. Rodriguez-Carvajal, *Recent Developments of the Program FULLPROF*, Commission on Powder Diffraction (IUCr). *Newsletter* 26 (2001) 12-19.
- [14] A.B. Velichenko, E.A. Baranova, D.V. Girenko, R. Amadelli, S.V. Kovalyov, F.I. Danilov, *Russ. J. Electrochem.* 39 (2003) 615-621.
- [15] O. Shmychkova, T. Luk'yanenko, R. Amadelli, A. Velichenko, *J. Electroanal. Chem.* 774 (2016) 88-94.
- [16] X. Li, D. Pletcher, F.C. Walsh, *Chem. Soc. Rev.* 40(7) (2011) 3879-3894.
- [17] I. Petersson, E. Ahlberg, B. Berghult, *J. Power Sources* 76 (1998) 98-105.
- [18] O. Shmychkova, T. Luk'yanenko, A. Piletska, A. Velichenko, R. Gladyshevskii, P. Demchenko, R. Amadelli, *J. Electroanal. Chem.* 746 (2015) 57-61.
- [19] T. Luk'yanenko, A. Velichenko, V. Knysh, O. Shmychkova, *Vopr. Khim. Khim. Tekhnol.* 4 (2018) 27-35.